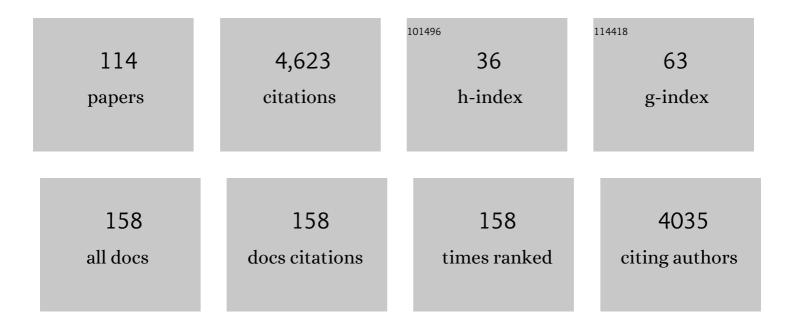
List of Publications by Year in descending order

Source: https://exaly.com/author-pdf/5955914/publications.pdf Version: 2024-02-01



#	Article	IF	CITATIONS
1	Seismic Imaging of the Downwelling Indian Lithosphere Beneath Central Tibet. Science, 2003, 300, 1424-1427.	6.0	310
2	Gradual unlocking of plate boundary controlled initiation of the 2014 Iquique earthquake. Nature, 2014, 512, 299-302.	13.7	279
3	Tibetan plate overriding the Asian plate in central and northern Tibet. Nature Geoscience, 2011, 4, 870-873.	5.4	202
4	Seismic polarization anisotropy beneath the central Tibetan Plateau. Journal of Geophysical Research, 2000, 105, 27979-27989.	3.3	181
5	Mapping the Hawaiian plume conduit with converted seismic waves. Nature, 2000, 405, 938-941.	13.7	174
6	Deep India meets deep Asia: Lithospheric indentation, delamination and break-off under Pamir and Hindu Kush (Central Asia). Earth and Planetary Science Letters, 2016, 435, 171-184.	1.8	148
7	The AlpArray Seismic Network: A Large-Scale European Experiment to Image the Alpine Orogen. Surveys in Geophysics, 2018, 39, 1009-1033.	2.1	138
8	The 2015 Illapel earthquake, central Chile: A type case for a characteristic earthquake?. Geophysical Research Letters, 2016, 43, 574-583.	1.5	120
9	A complex Tibetan upper mantle: A fragmented Indian slab and no south-verging subduction of Eurasian lithosphere. Earth and Planetary Science Letters, 2012, 333-334, 101-111.	1.8	117
10	Rayleigh wave phase velocity maps of Tibet and the surrounding regions from ambient seismic noise tomography. Geochemistry, Geophysics, Geosystems, 2010, 11, .	1.0	105
11	Complex hazard cascade culminating in the Anak Krakatau sector collapse. Nature Communications, 2019, 10, 4339.	5.8	105
12	Crustal structure of northern and southern Tibet from surface wave dispersion analysis. Journal of Geophysical Research, 2003, 108, .	3.3	96
13	Coalescence microseismic mapping. Geophysical Journal International, 2013, 195, 1773-1785.	1.0	95
14	Seismic evidence for stratification in composition and anisotropic fabric within the thick lithosphere of Kalahari Craton. Geochemistry, Geophysics, Geosystems, 2013, 14, 5393-5412.	1.0	85
15	Aftershock seismicity of the 27 February 2010 Mw 8.8 Maule earthquake rupture zone. Earth and Planetary Science Letters, 2012, 317-318, 413-425.	1.8	80
16	A high-resolution, time-variable afterslip model for the 2010 Maule Mw = 8.8, Chile megathrust earthquake. Earth and Planetary Science Letters, 2013, 383, 26-36.	1.8	78
17	Structure and seismogenic properties of the Mentawai segment of the Sumatra subduction zone revealed by local earthquake traveltime tomography. Journal of Geophysical Research, 2012, 117, .	3.3	76
18	SMART Cables for Observing the Global Ocean: Science and Implementation. Frontiers in Marine Science, 2019. 6.	1.2	73

#	Article	IF	CITATIONS
19	Thickness of the lithosphere beneath Turkey and surroundings from S-receiver functions. Solid Earth, 2015, 6, 971-984.	1.2	72
20	Which Picker Fits My Data? A Quantitative Evaluation of Deep Learning Based Seismic Pickers. Journal of Geophysical Research: Solid Earth, 2022, 127, .	1.4	66
21	The Fine Structure of the Subducted Investigator Fracture Zone in Western Sumatra as Seen by Local Seismicity. Earth and Planetary Science Letters, 2010, 298, 47-56.	1.8	64
22	The September 2009 Padang earthquake. Nature Geoscience, 2010, 3, 70-71.	5.4	62
23	Subducted seafloor relief stops rupture in South American great earthquakes: Implications for rupture behaviour in the 2010 Maule, Chile earthquake. Earth and Planetary Science Letters, 2010, 298, 89-94.	1.8	62
24	Shear-wave structure of the lithosphere above the Hawaiian Hot Spot from two-station Rayleigh wave phase velocity measurements. Geophysical Research Letters, 1999, 26, 1493-1496.	1.5	58
25	Seismicity and geometry of the south Chilean subduction zone (41.5°S–43.5°S): Implications for controlling parameters. Geophysical Research Letters, 2007, 34, .	1.5	55
26	Fibre optic distributed acoustic sensing of volcanic events. Nature Communications, 2022, 13, 1753.	5.8	54
27	About the lithospheric structure of central Tibet, based on seismic data from the INDEPTH III profile. Tectonophysics, 2004, 380, 1-25.	0.9	52
28	Insight into NE Tibetan Plateau expansion from crustal and upper mantle anisotropy revealed by shear-wave splitting. Earth and Planetary Science Letters, 2017, 478, 66-75.	1.8	49
29	The transformer earthquake alerting model: a new versatile approach to earthquake early warning. Geophysical Journal International, 2021, 225, 646-656.	1.0	49
30	Relationship between the upper mantle high velocity seismic lid and the continental lithosphere. Lithos, 2009, 109, 112-124.	0.6	47
31	Significant and vertically coherent seismic anisotropy beneath eastern Tibet. Journal of Geophysical Research, 2012, 117, .	3.3	46
32	Depthâ€variant azimuthal anisotropy in Tibet revealed by surface wave tomography. Geophysical Research Letters, 2015, 42, 4326-4334.	1.5	46
33	Fragmented Indian plate and vertically coherent deformation beneath eastern Tibet. Journal of Geophysical Research, 2012, 117, .	3.3	44
34	The Crust in the Pamir: Insights From Receiver Functions. Journal of Geophysical Research: Solid Earth, 2019, 124, 9313-9331.	1.4	42
35	Field observations of seismic velocity changes caused by shaking-induced damage and healing due to mesoscopic nonlinearity. Geophysical Journal International, 2016, 204, 1490-1502.	1.0	41
36	A 3D shear-wave velocity model of the upper mantle beneath China and the surrounding areas. Tectonophysics, 2014, 633, 193-210.	0.9	40

#	Article	IF	CITATIONS
37	P-wave velocity structure of the uppermost mantle beneath Hawaii from traveltime tomography. Geophysical Journal International, 2001, 146, 594-606.	1.0	38
38	Seismicity in the outer rise offshore southern Chile: Indication of fluid effects in crust and mantle. Earth and Planetary Science Letters, 2008, 269, 41-55.	1.8	37
39	Earthquake magnitude and location estimation from real time seismic waveforms with a transformer network. Geophysical Journal International, 2021, 226, 1086-1104.	1.0	37
40	Crustal structure of the British Isles and its epeirogenic consequences. Geophysical Journal International, 2012, 190, 705-725.	1.0	36
41	Seismic Broadband Ocean-Bottom Data and Noise Observed with Free-Fall Stations: Experiences from Long-Term Deployments in the North Atlantic and the Tyrrhenian Sea. Bulletin of the Seismological Society of America, 2006, 96, 647-664.	1.1	35
42	The structure of the Sumatran Fault revealed by local seismicity. Geophysical Research Letters, 2012, 39, .	1.5	34
43	Splay fault activity revealed by aftershocks of the 2010 Mw 8.8 Maule earthquake, central Chile. Geology, 2014, 42, 823-826.	2.0	33
44	SeisBench—A Toolbox for Machine Learning in Seismology. Seismological Research Letters, 2022, 93, 1695-1709.	0.8	32
45	Microearthquake seismicity of the Mid-Atlantic Ridge at 5°S: A view of tectonic extension. Journal of Geophysical Research, 2004, 109, .	3.3	31
46	Seismic anisotropy in the Sumatra subduction zone. Journal of Geophysical Research: Solid Earth, 2013, 118, 5372-5390.	1.4	29
47	The structure of the crust and uppermost mantle beneath Madagascar. Geophysical Journal International, 2017, 210, 1525-1544.	1.0	29
48	Comparison of postseismic afterslip models with aftershock seismicity for three subduction-zone earthquakes: Nias 2005, Maule 2010 and Tohoku 2011. Geophysical Journal International, 2014, 199, 784-799.	1.0	28
49	Imaging the lithosphere beneath NE Tibet: teleseismic P and S body wave tomography incorporating surface wave starting models. Geophysical Journal International, 2014, 196, 1724-1741.	1.0	27
50	The updip seismic/aseismic transition of the Sumatra megathrust illuminated by aftershocks of the 2004 Aceh-Andaman and 2005 Nias events. Geophysical Journal International, 2010, , .	1.0	26
51	Scandinavia: A former Tibet?. Geochemistry, Geophysics, Geosystems, 2013, 14, 4479-4487.	1.0	25
52	Seismic Anisotropy from SKS Splitting beneath Northeastern Tibet. Bulletin of the Seismological Society of America, 2013, 103, 3362-3371.	1.1	25
53	Crustal structure of southern Madagascar from receiver functions and ambient noise correlation: Implications for crustal evolution. Journal of Geophysical Research: Solid Earth, 2017, 122, 1179-1197.	1.4	24
54	High-frequency seismic radiation from Maule earthquake (Mw 8.8, 2010 February 27) inferred from high-resolution backprojection analysis. Geophysical Journal International, 2014, 199, 1058-1077.	1.0	23

#	Article	IF	CITATIONS
55	Probing the Northern Chile Megathrust With Seismicity: The 2014 M8.1 Iquique Earthquake Sequence. Journal of Geophysical Research: Solid Earth, 2019, 124, 12935-12954.	1.4	23
56	Magmatic and Sedimentary Structure beneath the Klyuchevskoy Volcanic Group, Kamchatka, From Ambient Noise Tomography. Journal of Geophysical Research: Solid Earth, 2020, 125, e2019JB018900.	1.4	23
57	Shear wave splitting and mantle flow beneath LA RISTRA. Geophysical Research Letters, 2003, 30, .	1.5	22
58	Seismic anisotropy of the lithosphere and asthenosphere beneath southern Madagascar from teleseismic shear wave splitting analysis and waveform modeling. Journal of Geophysical Research: Solid Earth, 2016, 121, 6627-6643.	1.4	22
59	Full Waveform Inversion Beneath the Central Andes: Insight Into the Dehydration of the Nazca Slab and Delamination of the Backâ€Arc Lithosphere. Journal of Geophysical Research: Solid Earth, 2021, 126, e2021JB021984.	1.4	21
60	Structure of the central Sumatran subduction zone revealed by local earthquake travel-time tomography using an amphibious network. Solid Earth, 2018, 9, 1035-1049.	1.2	20
61	Modification of the Seismic Properties of Subducting Continental Crust by Eclogitization and Deformation Processes. Journal of Geophysical Research: Solid Earth, 2019, 124, 9731-9754.	1.4	20
62	Shear velocity structure across the Sumatran Forearc-Arc. Geophysical Journal International, 2012, 189, 1306-1314.	1.0	19
63	Ambientâ€noise tomography of north Tibet limits geological terrane signature to upperâ€middle crust. Geophysical Research Letters, 2013, 40, 808-813.	1.5	19
64	The Interplay of Eclogitization and Deformation During Deep Burial of the Lower Continental Crust—A Case Study From the Bergen Arcs (Western Norway). Tectonics, 2019, 38, 898-915.	1.3	19
65	Crustal structure of a rifted oceanic core complex and its conjugate side at the MAR at 5°S: implications for melt extraction during detachment faulting and core complex formation. Geophysical Journal International, 2010, 181, 113-126.	1.0	17
66	Crustal Radial Anisotropy and Linkage to Geodynamic Processes: A Study Based on Seismic Ambient Noise in Southern Madagascar. Journal of Geophysical Research: Solid Earth, 2018, 123, 5130-5146.	1.4	17
67	Subduction system variability across the segment boundary of the 2004/2005 Sumatra megathrust earthquakes. Earth and Planetary Science Letters, 2013, 365, 108-119.	1.8	16
68	Investigation of mantle kinematics beneath the Hellenic-subduction zone with teleseismic direct shear waves. Physics of the Earth and Planetary Interiors, 2016, 261, 141-151.	0.7	16
69	<i>P</i> Wave Azimuthal Anisotropic Tomography in Northern Chile: Insight Into Deformation in the Subduction Zone. Journal of Geophysical Research: Solid Earth, 2019, 124, 742-765.	1.4	16
70	Infragravity wave source regions determined from ambient noise correlation. Geophysical Research Letters, 2012, 39, .	1.5	15
71	3â€D active source tomography around Simeulue Island offshore Sumatra: Thick crustal zone responsible for earthquake segment boundary. Geophysical Research Letters, 2013, 40, 48-53.	1.5	15
72	The Use of Direct Shear Waves in Quantifying Seismic Anisotropy: Exploiting Regional Arrays. Bulletin of the Seismological Society of America, 2014, 104, 2644-2661.	1.1	14

#	Article	IF	CITATIONS
73	Low uncertainty multifeature magnitude estimation with 3-D corrections and boosting tree regression: application to North Chile. Geophysical Journal International, 2020, 220, 142-159.	1.0	14
74	Constraints on crustal and mantle structure of the oceanic plate south of Iceland from ocean bottom recorded Rayleigh waves. Tectonophysics, 2008, 447, 66-79.	0.9	13
75	Seismic Anisotropy Beneath the Pamir and the Hindu Kush: Evidence for Contributions From Crust, Mantle Lithosphere, and Asthenosphere. Journal of Geophysical Research: Solid Earth, 2018, 123, 10,727.	1.4	13
76	The GEOFON Program in 2020. Seismological Research Letters, 2021, 92, 1610-1622.	0.8	13
77	Seismology Across the Northeastern Edge of the Tibetan Plateau. Eos, 2008, 89, 487-487.	0.1	12
78	Application of multichannel Wiener filters to the suppression of ambient seismic noise in passive seismic arrays. The Leading Edge, 2008, 27, 232-238.	0.4	12
79	Role of Serpentinized Mantle Wedge in Affecting Megathrust Seismogenic Behavior in the Area of the 2010 <i>M</i> = 8.8 Maule Earthquake. Geophysical Research Letters, 2020, 47, e2020GL090482.	1.5	12
80	Crustal Structure of Sri Lanka Derived From Joint Inversion of Surface Wave Dispersion and Receiver Functions Using a Bayesian Approach. Journal of Geophysical Research: Solid Earth, 2020, 125, e2019JB018688.	1.4	12
81	The SWATH-D Seismological Network in the Eastern Alps. Seismological Research Letters, 2021, 92, 1592-1609.	0.8	12
82	Shear wave splitting in the Alpine region. Geophysical Journal International, 2021, 227, 1996-2015.	1.0	12
83	Application of frequency-dependent multichannel Wiener filters to detect events in 2D three-component seismometer arrays. Geophysics, 2009, 74, V133-V141.	1.4	11
84	Upper-mantleP- andS-wave velocities across the Northern Tornquist Zone from traveltime tomography. Geophysical Journal International, 2015, 203, 437-458.	1.0	11
85	Systematic Changes of Earthquake Rupture with Depth: A Case Study from the 2010 <i>M</i> <sub>w</sub> A8.8 Maule, Chile, Earthquake Aftershock Sequence. Bulletin of the Seismological Society of America, 2015, 105, 2468-2479.	1.1	10
86	Receiver-function imaging of the lithosphere at the Kunlun-Qaidam boundary, Northeast Tibet. Tectonophysics, 2019, 759, 30-43.	0.9	10
87	Another look at the treatment of data uncertainty in Markov chain Monte Carlo inversion and other probabilistic methods. Geophysical Journal International, 2020, 222, 388-405.	1.0	10
88	PandSwave scattering from mantle plumes. Journal of Geophysical Research, 1998, 103, 21145-21163.	3.3	9
89	Revision of earthquake hypocentre locations in global bulletin data sets using source-specific station terms. Geophysical Journal International, 2017, 208, 589-602.	1.0	9
90	ScanArray—A Broadband Seismological Experiment in the Baltic Shield. Seismological Research Letters, 2021, 92, 2811-2823.	0.8	9

#	Article	IF	CITATIONS
91	Exploring Structural Controls on Sumatran Earthquakes. Eos, 2010, 91, 405-406.	0.1	8
92	Joint ambient noise autocorrelation and receiver function analysis of the Moho. Geophysical Journal International, 2021, 225, 1920-1934.	1.0	8
93	Application of the Multichannel Wiener Filter to Regional Event Detection Using NORSAR Seismic-Array Data. Bulletin of the Seismological Society of America, 2011, 101, 2887-2896.	1.1	7
94	Advancing Subduction Zone Science After a Big Quake. Eos, 2014, 95, 193-194.	0.1	7
95	<i>P</i> Wave Anisotropy Caused by Partial Eclogitization of Descending Crust Demonstrated by Modeling Effective Petrophysical Properties. Geochemistry, Geophysics, Geosystems, 2020, 21, e2019GC008906.	1.0	7
96	Seismic anisotropy and mantle deformation in NW Iran inferred from splitting measurements of SK(K)S and direct S phases. Geophysical Journal International, 2021, 226, 1417-1431.	1.0	7
97	Impact of the Juan Fernandez Ridge on the Pampean Flat Subduction Inferred From Full Waveform Inversion. Geophysical Research Letters, 2021, 48, e2021GL095509.	1.5	7
98	Commercial Underwater Cable Systems Could Reduce Disaster Impact. Eos, 2017, , .	0.1	6
99	Editorialâ€~Submarine geomorphology: new views on an â€~unseen' landscape. Basin Research, 2008, 20, 467-472.	1.3	5
100	Applicability and Bias ofVP/VSEstimates byPandSDifferential Arrival Times of Spatially Clustered Earthquakes. Bulletin of the Seismological Society of America, 2016, 106, 1055-1063.	1.1	5
101	Seismic structure across central Myanmar from joint inversion of receiver functions and Rayleigh wave dispersion. Tectonophysics, 2021, 818, 229068.	0.9	5
102	Estimating Rupture Directions from Local Earthquake Data Using the IPOC Observatory in Northern Chile. Seismological Research Letters, 2018, 89, 495-502.	0.8	5
103	Imaging the Ethiopian Rift Region Using Transdimensional Hierarchical Seismic Noise Tomography. Pure and Applied Geophysics, 2021, 178, 4367-4388.	0.8	5
104	Anomalous azimuthal variations with 360° periodicity of Rayleigh phase velocities observed in Scandinavia. Geophysical Journal International, 2020, 224, 1684-1704.	1.0	5
105	A Probabilistic View on Rupture Predictability: All Earthquakes Evolve Similarly. Geophysical Research Letters, 2022, 49, .	1.5	5
106	Crustal structure and kinematics of the TAMMAR propagating rift system on the Mid-Atlantic Ridge from seismic refraction and satellite altimetry gravity. Geophysical Journal International, 2016, 206, 1382-1397.	1.0	4
107	Continental Breakâ€Up Under a Convergent Setting: Insights From P Wave Radial Anisotropy Tomography of the Woodlark Rift in Papua New Guinea. Geophysical Research Letters, 2022, 49, .	1.5	3
108	Velocity structure and radial anisotropy of the lithosphere in southern Madagascar from surface wave dispersion. Geophysical Journal International, 2020, 224, 1930-1944.	1.0	2

#	Article	IF	CITATIONS
109	UNIBRA/DSEBRA: The German Seismological Broadband Array and Its Contribution to AlpArray—Deployment and Performance. Seismological Research Letters, 0, , .	0.8	2
110	Seismic velocity and anisotropy of the uppermost mantle beneath Madagascar from <i>Pn</i> tomography. Geophysical Journal International, 2020, 224, 290-305.	1.0	1
111	Comment on "Potential shortâ€ŧerm earthquake forecasting by farm animal monitoring―by Wikelski, Mueller, Scocco, Catorci, Desinov, Belyaev, Keim, Pohlmeier, Fechteler, and Mai. Ethology, 2021, 127, 302-306.	0.5	1
112	Submarine Cable Systems for Future Societal Needs. Eos, 2016, 97, .	0.1	1
113	Crustal Structure of the Indochina Peninsula From Ambient Noise Tomography. Journal of Geophysical Research: Solid Earth, 2022, 127, .	1.4	1
114	LEE, W. H. K., KANAMORI, H., JENNINGS, P. C. & KISSLINGER, C. (eds) 2002. International Handbook of Earthquake & Engineering Seismology, Part A. International Geophysics Series Volume 81A. xliii + 933 pp. + CD-ROM. Amsterdam, Boston, London, New York: Academic Press (Elsevier Science) in conjunction with the International Association of Seismology and Physics of the Earth's Interior (IASPEI). Price £100.00 (hard covers). ISBN 0 12 440652 1. Geological Magazine, 2004, 141, 744-745.	0.9	0